Raman study of coupled-phonon–crystal-field excitations in $Nd_{1+x}Ba_{2-x}Cu_3O_y$ single crystals

A. A. Martin, T. Ruf, T. Strach, and M. Cardona
Max-Planck-Institut für Festkörperforschung, Heisenbergstraße 1, D-70569 Stuttgart, Germany

T. Wolf
Forschungszentrum Karlsruhe, Institut für Technische Physik, D-76021 Karlsruhe, Germany
(Received 9 June 1998)

We study effects due to Nd^{3+}/Ba^{2+} ion substitution in $Nd_{1+x}Ba_{2-x}Cu_3O_y$ single crystals ($0.00 \leqslant x \leqslant 0.33$ and $6.0 \leqslant y \leqslant 7.0$) using Raman scattering from coupled-phonon–crystal-field (CF) excitations. At low temperature the B_{1g} phonon [O(2)-O(3) out-of-phase vibration in the CuO_2 planes] interacts with a nearby CF excitation of the Nd^{3+} $4f$ electrons resulting in a double-peak structure. Systematic changes of the peak frequencies and their relative intensities occur as a function of x and y. Using a two-level model we calculate from the Raman spectra the unrenormalized B_{1g} phonon and CF excitation energies as well as the coupling constant. In three series of experiments ($y \sim 7.0$, varying x; $y \sim 6.0$, varying x; $x = 0$, varying y) we observe different but consistent changes of the superconductivity-induced B_{1g} phonon softenings with temperature. These changes suggest that the superconducting gap in the underdoped region continues to increase with respect to the phonon energy, even if T_c decreases. At room temperature the frequency of the B_{1g} phonon hardly changes with doping. We also observe variations in the CF excitation energies that are discussed in terms of structural changes and charge transfer between reservoirs (e.g., in the chains) and the oxygen ions in the CuO_2 planes. [S0163-1829(98)01345-9]

I. INTRODUCTION

It is well known that the hole concentration plays a crucial role in the superconducting properties of the perovskite high-temperature superconductors. In $RBa_2Cu_3O_{7-y}$ (R=Y and most rare-earth atoms), a change in the hole concentration can be achieved, among other possibilities, by either removing or adding oxygen or by placing trivalent ions on the Ba crystallographic sites. As far as the latter approach is concerned, several studies have been devoted to $Nd_{1+x}Ba_{2-x}Cu_3O_y$, in which Nd^{3+} has a large solubility into the Ba^{2+} site, thus allowing for a large degree of substitution without forming second phases.[1–5] The replacement of Ba^{2+} by Nd^{3+} has two major effects:[3] (i) it leads to a structural change from orthorhombic to tetragonal for $x \geqslant 0.25$, and (ii) it increases the electron concentration in the CuO_2 planes, thereby decreasing the superconducting transition temperature T_c from 95 K ($x=0.0$, $y=7.0$) to 6 K ($x=0.33$, $y=7.0$).

In $Nd_{1+x}Ba_{2-x}Cu_3O_y$, the O(2)-O(3) out-of-phase vibration of the CuO_2 planes, found in the Raman spectra of the $RBa_2Cu_3O_y$ series around 300 cm^{-1}, has B_{1g} symmetry in the approximate tetragonal D_{4h} point group. This mode interacts with a nearby B_{1g} transition between two crystal-field (CF) levels of the Nd^{3+} ($J=9/2$) ground-state multiplet. Due to this coupling, the B_{1g} phonon splits into a double peak at low temperature, which can be observed by Raman[6,7] or inelastic neutron scattering.[8] The CF levels are very sensitive to ligands in the immediate vicinity of the rare-earth (RE) ions that are located between the CuO_2 planes. Therefore their changes with doping, temperature, pressure, or magnetic field can be used to study phenomena related to high-temperature superconductivity such as, for example, the charge transferred between the chains and oxygen ions in the CuO_2 planes.[4,9,10]

Recently, coupled-phonon-CF excitations have been studied by Raman scattering in a series of $NdBa_2Cu_{3-x}Ga_xO_7$ ceramics.[10] From fits of a two-level model to the renormalized line shapes, the bare phonon and CF frequencies as well as the coupling constant were obtained. The observed shift of the CF excitation with Ga content x could be explained by structural changes and an increase of about 1% in the O(2) and O(3) charges for $x=0.08$ as compared to the Ga-free sample ($x=0.00$).[10] With respect to the resulting suppression of T_c, the charge transfer estimated from these experiments with Ga substitution is in qualitative agreement with earlier neutron studies where the oxygen content was varied.[4]

However, systematic experiments with the same method on a well-characterized set of samples are required in order to obtain a more general picture about the charge transfer and CF level shifts associated with different kinds of doping. We have therefore performed a Raman study of coupled-phonon-CF excitations in a series of very high quality $Nd_{1+x}Ba_{2-x}Cu_3O_y$ ($0.00 \leqslant x \leqslant 0.33$ and $6.0 \leqslant y \leqslant 7.0$) twinned single crystals. In these samples, T_c can be suppressed by varying both the Nd and the oxygen concentration. In addition, reference measurements on nonsuperconducting samples with $y=0.0$ are possible. Besides yielding information about CF levels, this approach also allows us to investigate superconductivity-induced phonon self-energy effects in a novel way: The B_{1g} phonon frequency in previous studies has been shifted with respect to the superconducting gap over a small range exploiting substitution effects.[11,12] In this work the phonon renormalization is studied over a wide range in the underdoped regime while the phonon frequency remains almost constant. This yields fur-

TABLE I. Superconducting transition temperatures T_c vs Nd content x and oxygen content y in the $Nd_{1+x}Ba_{2-x}Cu_3O_7$ and $NdBa_2Cu_3O_y$ samples used in the present investigation.

$Nd_{1+x}Ba_{2-x}Cu_3O_7$		$NdBa_2Cu_3O_y$	
x	T_c (K)	y	T_c (K)
0.00	95.0	7.0	95
0.12	69.5	6.9	88
0.20	40.0	6.8	60
0.25	32.0	6.6	40
0.33	6.0	6.4	
		6.0	

ther insight on the variation of the superconducting gap with doping.

II. EXPERIMENT

The $Nd_{1+x}Ba_{2-x}Cu_3O_y$ single crystals were grown by a self-flux method in Y-stabilized ZrO_2 crucibles starting from BaO ($BaCO_3$), Nd_2O_3, and CuO mixtures.[13] Crystal growth took place during slow cooling from 1040 °C to about 960 °C under different oxygen partial pressures. At the end of the growth process the remaining flux was either decanted within the furnace or sucked up by a porous piece of ceramic. Finally, the crystals were cooled down to room temperature by shutting off the furnace. The Nd/Ba ratio of the crystals grown in air could be varied by changing the Ba/Cu ratio of the flux. Crystals with a negligible amount of Nd/Ba substitution were grown under a pressure of 60 mbar of air, which was further reduced during cooling down to room temperature. After growth the crystals were oxidized for about 700 h in 1 bar oxygen between 600 °C and 300 °C. Reduced crystals were obtained by annealing at 700 °C for 95 h in an atmosphere of 1.8×10^{-5} bars of oxygen. The compositions of the single crystals were determined by energy-dispersive x-ray (EDX) measurements, and the oxygen content was derived from the weight change of the samples. The superconducting transition temperature was measured by dc magnetization for each combination of x and y. The results are presented in Table I. The single crystals with $y=6.4$ and 6.0 are not superconducting.

Raman spectra were recorded using a multichannel spectrometer equipped with a liquid-nitrogen-cooled charge-coupled-device (CCD) camera. The 514.5-nm line of an Ar-ion laser was used as an excitation source. The laser power at the sample was kept below 8 mW on a spot diameter of about 50 μm. The crystals were attached to the cold finger of a closed-cycle helium cryostat, held at a temperature of 10 K, and measured in a near-backscattering configuration on the a-b plane.

III. RESULTS

Polarized Raman spectra $[Z(XX)\overline{Z}]$ of $Nd_{1+x}Ba_{2-x}Cu_3O_7$ at 10 K, showing the dependence of the double-peak structure for different values of x, are presented in Fig. 1. For the lower-frequency peak we observe a small shift to lower energies and a decrease of its intensity relative to that of the higher-frequency peak with increasing x. The higher-frequency peak does not shift with x. We also find a pronounced broadening for both peaks with increasing x. From fits to these data using two Lorentzians and a linear background we obtain the frequencies of the lower- (ω_1) and higher-energy peak (ω_2) as well as their intensity ratio (R).

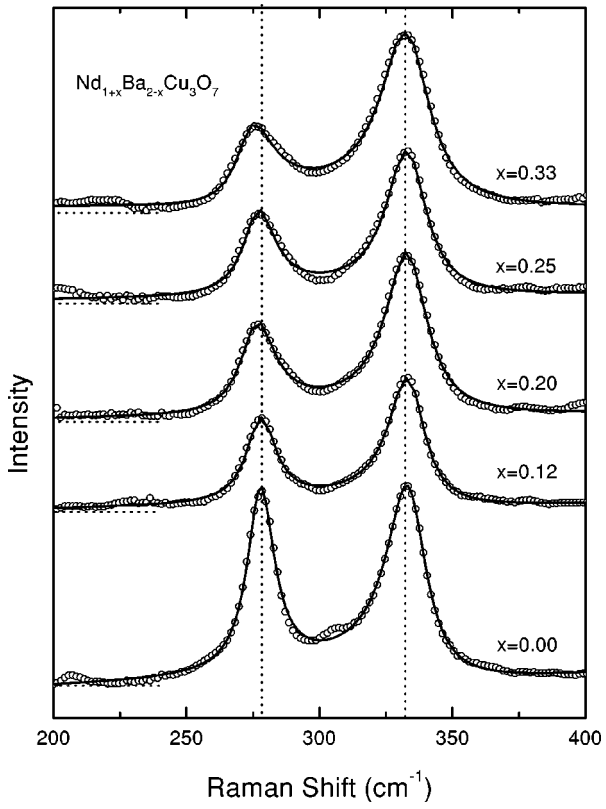

FIG. 1. Polarized Raman spectra in $Z(XX)\overline{Z}$ geometry for superconducting $Nd_{1+x}Ba_{2-x}Cu_3O_7$ at 10 K, showing the dependence of the double-peak structure for different values of x (open circles: data; solid lines: fits). The horizontal dashed lines indicate the respective base lines for the spectra that were vertically offset for clarity. The vertical dashed lines are to guide the eye.

In Fig. 2 we show polarized Raman spectra $[Z(XX)\overline{Z}]$ for the nonsuperconducting samples $Nd_{1+x}Ba_{2-x}Cu_3O_6$ with different values of x. With increasing x, the high-frequency peak exhibits a slight shift to lower frequencies, whereas the lower-frequency peak stays at the same energy. Note that this behavior is opposite to the one observed in Fig. 1. Both peaks show again a pronounced broadening with increasing x. Using the same fitting procedure as in Fig. 1, we have determined the values of ω_1, ω_2, and R.

Figure 3 displays Raman spectra of a third set of measurements on $NdBa_2Cu_3O_y$ single crystals in $Z(X'Y')\overline{Z}$ polarization at 10 K for different oxygen contents y. With decreasing y the lower-frequency peak shifts to lower energy, whereas the higher-frequency peak does not shift at all. The most pronounced frequency change occurs at $y=6.6$ when the macroscopic structural phase transition from orthorhombic to tetragonal takes place. The peaks at 232 and 266 cm^{-1}, which appear in the samples with $y=6.9$, 6.8, and 6.6, have been assigned previously to broken-chain modes.[14] They also appear for $y=6.4$, but with much less intensity. For the samples with $y=7.0$ and 6.0 they are absent. For $y>6.9$ and $y<6.6$ no appreciable change in fre-

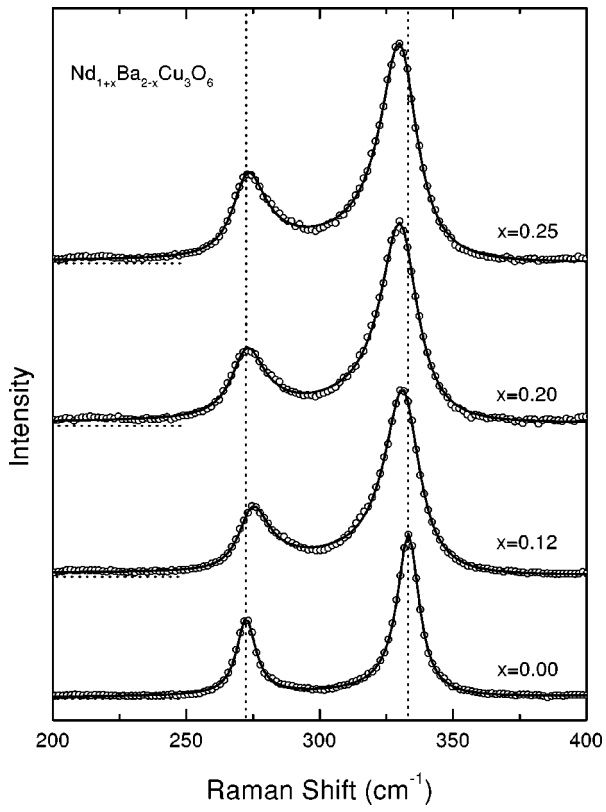

FIG. 2. Polarized Raman spectra in $Z(XX)\bar{Z}$ geometry for non-superconducting $Nd_{1+x}Ba_{2-x}Cu_3O_6$ at 10 K, showing the dependence of the double-peak structure for different values of x (labels as in Fig. 1).

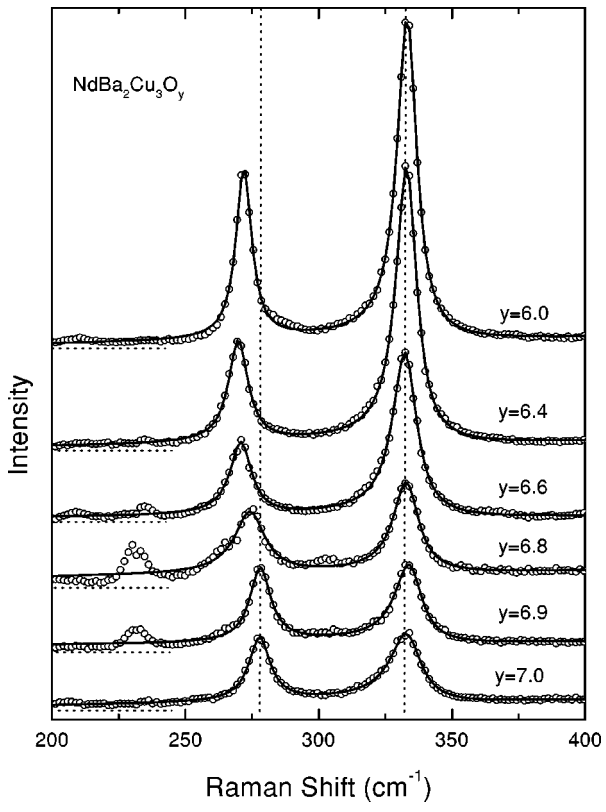

FIG. 3. Polarized Raman spectra in $Z(X'Y')\bar{Z}$ geometry of $NdBa_2Cu_3O_y$ at 10 K, showing the dependence of the double-peak structure for different values of y (labels as in Fig. 1).

quency is found in both components of the B_{1g} doublet. With decreasing y, we observe an intensity decrease of the lower-energy peak relative to that of the higher-energy peak. Using the same fitting procedure as described before we determined the values of ω_1, ω_2, and R.

IV. DISCUSSION

A. Determination of unrenormalized parameters

In $YBa_2Cu_3O_y$ the B_{1g} O(2)-O(3) out-of-phase phonon appears as a single peak whose frequency can be directly determined from fits to a Fano profile.[15] However, in $NdBa_2Cu_3O_y$, due to the phonon-CF excitation mixing, this phonon appears as a double peak at low temperature.[6–8] The unrenormalized frequencies of the CF excitation ω_{CF} and the phonon ω_{ph}, as well as the coupling constant V, can be obtained from ω_1, ω_2, and R with the following relations:[10,16,17]

$$\omega_{CF}=\frac{\omega_1+R\omega_2}{1+R}, \tag{1}$$

$$\omega_{ph}=\frac{R\omega_1+\omega_2}{1+R}, \tag{2}$$

and

$$V=|\omega_1-\omega_2|\frac{\sqrt{R}}{R+1}. \tag{3}$$

The low-temperature values for ω_{CF}, ω_{ph}, and V in $Nd_{1+x}Ba_{2-x}Cu_3O_7$, $Nd_{1+x}Ba_{2-x}Cu_3O_6$, and $NdBa_2Cu_3O_y$ calculated this way are shown in Figs. 4, 5, and 6, respectively. The room-temperature frequencies obtained from fits of the data to a single Fano profile are also plotted there. In principle, Fano profiles should also be used to fit the low-temperature data. However, residual inaccuracies of the model such as, e.g., the neglect of phonon and CF excitation dispersion effects, prevent a more detailed line-shape analysis of the two doublet components. We have therefore used only Lorentzians in the fits of Figs. 1–3.

In Fig. 4, the room-temperature frequency of the O(2)-O(3) phonon in fully oxygenated $Nd_{1+x}Ba_{2-x}Cu_3O_7$ is practically independent of x. However, at low temperature both the unrenormalized phonon and the bare CF frequencies show a strong dependence on x as the sample goes from normal to superconducting. At 10 K the phonon frequency for the sample with $x=0.00$ is about 7 cm^{-1} softer relative to its value at room temperature. In the range $0.00<x<0.33$ the magnitude of this phonon softening decreases almost linearly and vanishes for $x=0.33$. For the bare CF excitation the total energy decrease is about 8 cm^{-1} (2.7%) between $x=0.00$ and $x=0.33$. It varies almost linearly with x but seems to have a small step between $x=0.25$ (where the structural phase change occurs) and $x=0.33$. This step is also reflected by an abrupt change of the coupling constant in Fig. 4(b).

As can be seen in Fig. 5, the unrenormalized low-temperature phonon frequency in oxygen-depleted $Nd_{1+x}Ba_{2-x}Cu_3O_6$ is similar to the room-temperature value,

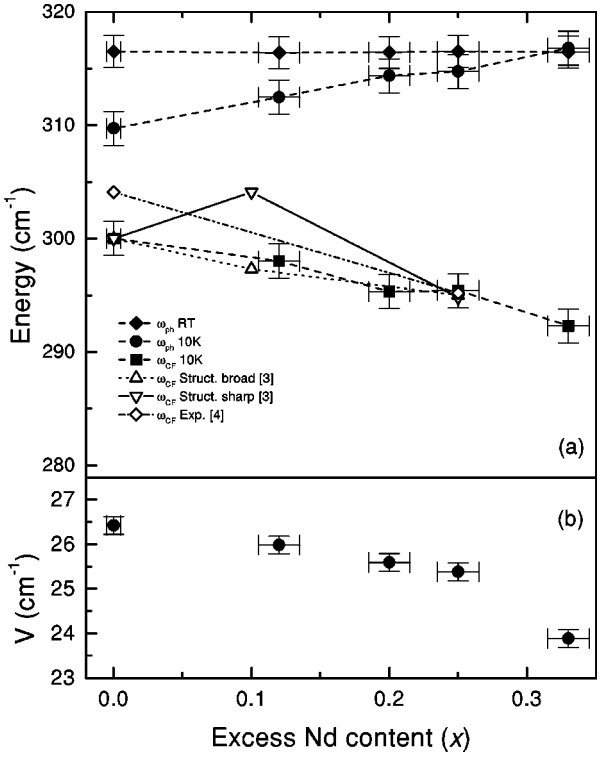

FIG. 4. Energies of (a) the unrenormalized phonon, the bare CF excitation, and (b) the coupling constant in superconducting $Nd_{1+x}Ba_{2-x}Cu_3O_7$ for different Nd contents x obtained from fits to the data in Fig. 1 (filled symbols: our data; open symbols: see text for details).

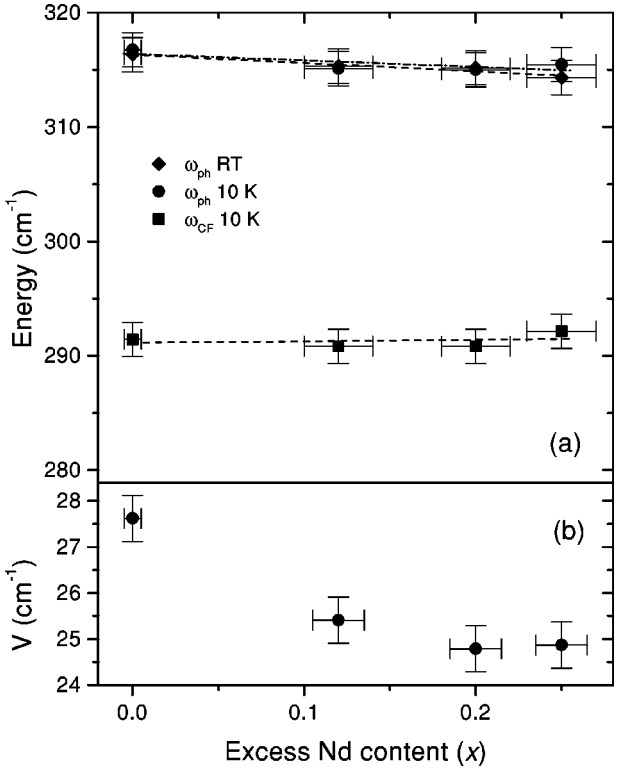

FIG. 5. Energies of (a) the unrenormalized phonon, the bare CF excitation and (b) the coupling constant in nonsuperconducting $Nd_{1+x}Ba_{2-x}Cu_3O_6$ for different Nd contents x obtained from fits to the data in Fig. 2 (filled symbols: our data).

i.e., no softening occurs between $x=0.00$ and 0.25. The bare CF energy also remains constant for these values of x. The coupling constant, shown in Fig. 5(b), is about 25 cm^{-1}, except for $x=0.00$, where it has the larger value of 27.6 cm^{-1}.

Figure 6 shows that the unrenormalized frequency of the B_{1g} phonon at room temperature is independent of the oxygen concentration within the error bars (316 ± 1.5 cm^{-1}). At 10 K, a decreasing oxygen content y in $NdBa_2Cu_3O_y$ has a similar effect on the unrenormalized CF and phonon energy as an increasing Nd concentration x in the fully oxygenated $Nd_{1+x}Ba_{2-x}Cu_3O_7$ samples. As the samples with $6.8<y<7.0$ go from normal to superconducting, the B_{1g} phonon softens by about (7 ± 1.5 cm^{-1}) relative to its frequency at room temperature. With decreasing y, the amount of phonon softening decreases almost linearly from $6.4<y<6.8$. For $y\leqslant6.4$ the softening vanishes. The maximum decrease of the bare CF energy is about 13 cm^{-1} (4.3%) in the range $6.0\leqslant y\leqslant7.0$. This change, however, appears to be nonlinear. From $y=7.0$ to $y=6.4$, ω_{CF} decreases strongly. For $y<6.4$ the data indicate a slight increase in ω_{CF} yielding a final total change of about 9 cm^{-1} (3.0%) compared to the value for $y=7.0$. In Fig. 6(b) we show the change in the coupling constant between $6.0\leqslant y\leqslant7.0$. A slight increase of V for decreasing oxygen content is observed. Note that the results for $x=0$ in Figs. 4 and 5 and $y=7.0$ in Fig. 6 are in good agreement with earlier investigations.[6,7,16,17]

B. Doping effects on phonons and CF excitations

From Figs. 4–6 we identify three main effects. First, the amount of phonon softening in the superconducting samples decreases in a similar way with both increasing x and decreasing y, i.e., it correlates with T_c. Second, ω_{CF} in the superconducting samples decreases with increasing x and decreasing y. Third, both the phonon softening and the variation of ω_{CF} with changing x or y vanish in the nonsuperconducting samples.

1. Superconducting samples: Phonon self-energy effects

Concerning the change in the amount of the phonon softening with doping, it is known that for the fully oxidized $Nd_{1+x}Ba_{2-x}Cu_3O_7$ samples increasing x decreases the hole concentration in the CuO_2 planes.[1–5] The additional Nd^{3+} ions on the Ba sites create chain-oxygen disorder and negative charges.[3] Acting together, these effects may cancel holes in the CuO_2 planes. Therefore, the compound becomes more underdoped with increasing x, and T_c decreases. The observed decrease in the amount of phonon softening with increasing x reflects changes in the real part of the phonon self-energy that have been described, e.g., by strong-coupling BCS theory.[18] This theory predicts that phonon self-energy effects change strongly, depending on the location of the gap relative to the energy of the phonon. In particular, a phonon should soften or harden below T_c, depending on whether it is located below or above the superconducting gap.[11]

This picture qualitatively explains the observed changes in the phonon softening in Figs. 4 and 6 for $Nd_{1+x}Ba_{2-x}Cu_3O_7$ and $NdBa_2Cu_3O_y$. Figure 6 indicates that for the $NdBa_2Cu_3O_y$ samples the maximum phonon softening occurs around $y=6.9$. For these values of y the gap

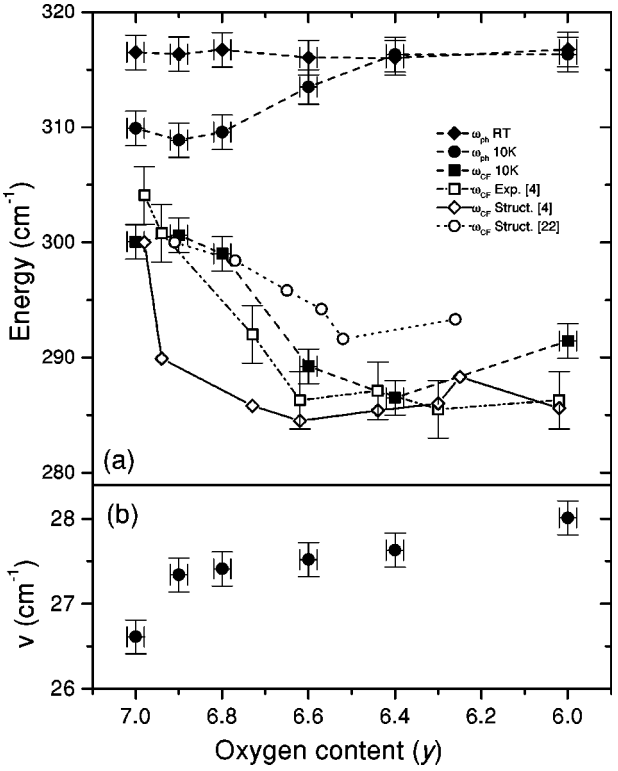

FIG. 6. Energies of (a) the unrenormalized phonon, the bare CF excitation and (b) the coupling constant in $NdBa_2Cu_3O_y$ for different oxygen contents y obtained from fits to the data in Fig. 3 (filled symbols: our data; open symbols: see text for details).

energy is very near to the B_{1g} mode, and the effect on the real part of the phonon self-energy is close to its maximum.[11,12,18] As the gap moves away from the B_{1g} phonon towards higher energies one expects the softening to become weaker. This is well reflected by the reduced phonon softening observed with decreasing y (Fig. 6) and also with increasing x (Fig. 4). For phonon frequencies far above the gap and with the sample still superconducting (large x in Fig. 4, small y in Fig. 6) a slight mode hardening is expected from the theory of Ref. 18, as has been observed for the O(2)-O(3) in-phase vibration of the CuO_2 planes.[11,12] However, this behavior is not observed here for the O(2)-O(3) out-of-phase phonon. We conjecture that absence of phonon hardening under these condictions is consistent with recent reports from $Bi_2Sr_2CaCu_2O_{8+y}$ that the superconducting gap in the underdoped regime continues to increase even if T_c decreases.[19,20] In such a scenario the softening would vanish due to the increasing separation in energy between the B_{1g} phonon and the coupling peak in the electronic excitation spectrum. Note that the relation of phonon self-energy effects with superconductivity, which has been established in Raman experiment under high magnetic fields,[21] needs to be reinvestigated in view of these new ideas. In Fig. 5, the B_{1g} phonon does not exhibit any shift attributable to self-energy effects. This is consistent with the fact that these samples are not superconducting.

Note that the present approach is complementary to earlier investigations where phonon self-energy effects have been probed by tuning the B_{1g} phonon frequency (e.g., by rare-earth or isotope substitution) across a gap that remained almost constant.[11,12] Furthermore, the softening in Fig. 6 remains clearly visible for smaller y as long as the sample is superconducting. In earlier studies,[22–24] the softening in $YBa_2Cu_3O_{7-y}$ was found to vanish for small deviations from optimal doping even though the samples were still superconducting. This apparent difference also calls for futher investigations.

2. Superconducting samples: Effects on CF levels

In Figs. 4 and 6, ω_{CF} decreases with either increasing x or decreasing y. These changes cannot be due to charge transfer mediated by the Nd^{3+} ions on the Ba sites (Fig. 4) or oxygen ions in the chains (Fig. 6) to the O(2) and O(3) oxygens in the CuO_2 planes alone, since one would then expect an increase of the CF energy due to the increase of the local electric field at the position of the RE ion.[10] In order to account for the observations one should therefore also consider a contribution due to structural changes. Doping affects the oxygen ligand geometry around the central Nd^{3+} ions, and any such changes are reflected directly in the CF levels. Such effects can be described by the point-charge model that allows one to calculate changes of the CF parameters, used to compute CF energy levels, from the positions and charges of the surrounding ligands of the RE ion.[4,10,25] This requires precise structural information, e.g., from neutron-diffraction experiments. In the case of $RBa_2Cu_3O_7$-type high-temperature superconductors one usually considers only the positions of the eight oxygens surrounding the Nd^{3+} ions in order to evaluate effects due to structural changes and charge transfer.[4,10]

Due to the lack of neutron-diffraction data for our (small) samples, we have performed such calculations using structural data available in the literature for similar compounds.[1,3,4,26] The data from Refs. 1 and 3 are for different Ba concentrations x in fully oxygenated superconducting $Nd_{1+x}Ba_{2-x}Cu_3O_7$. The results of a point-charge model calculation with the data of Ref. 3 for samples with ''sharp'' or ''broad'' superconducting transitions qualitatively show a decrease of ω_{CF} with increasing x (open triangles in Fig. 4). The calculated CF level energies were scaled to $\omega_{CF} = 300$ cm^{-1} for the ''sharp'' transition sample with $x = 0.0$.[27] CF levels calculated with the structural data from Ref. 1 (not included in Fig. 4) have the correct magnitude; however, these data are not precise enough. The CF levels vary a lot with x without exhibiting any clear trend. Two experimental values for $x = 0.0$ and 0.25, obtained from fits to CF level spectra in Ref. 4 (see Table II of Ref. 4), are also included (open diamonds). While our experimental results confirm the trend observed in Ref. 4 with better accuracy, the considerable scatter in the calculated CF level energies prohibits the separation of doping effects into structural and charge-transfer contributions. The main reason for this stems from the uncertainty in the z coordinates of the O(2) and O(3) ions that leads to large error bars in the calculated crystal-field levels. It appears, however, that most of the decrease of ω_{CF} with Ba content x is caused by structural effects.

Table II of Ref. 4 also presents fitted CF levels for $NdBa_2Cu_3O_y$ with different oxygen contents y. These experimental values of ω_{CF} are shown as open squares in Fig. 6(a). Again, our Raman data (filled squares) confirm the results of Ref. 4 with improved precision. From the atomic positions

given in Table I of Ref. 4 we have calculated the expected shift of the CF level due to structural changes alone. These results, scaled to $\omega_{CF}=300\ \mathrm{cm}^{-1}$ for $y=7.0$,[27] are given by the open diamonds in Fig. 6(a). Their deviation from the experimental data in the range $6.6\leqslant y\leqslant 7.0$ indicates a charge-transfer contribution to ω_{CF}. However, more precise structural data are necessary to quantify this effect. This necessity is underlined by calculations using the positional data given in Ref. 26. The results are shown by the open circles in Fig. 6(a). While following the same general trend, a reduction of ω_{CF} with decreasing y, these data are even somewhat higher than the experimental data, thus suggesting a charge transfer that would not have the correct sign.

3. Nonsuperconducting samples

In Fig. 5 we show values of ω_{CF} for nonsuperconducting $Nd_{1+x}Ba_{2-x}Cu_3O_6$ samples. The bare CF level energy remains constant for all Ba concentrations x. This observation appears unusual at first sight, since structural and charge modifications due to excess Nd ions on Ba sites should affect the CF levels in a similar way as in Fig. 4, independent of the oxygen concentration. However, this phenomenon can be made plausible in view of the results from Ref. 3, where a model was proposed in which the charge transfer from the chains to the planes depends on the amount of fourfold-planar-coordinated Cu(1) chain sites. For $Nd_{1+x}Ba_{2-x}Cu_3O_7$, the number of such sites decreases due to chain-oxygen disorder introduced by excess Nd.[3] This reduces the chain-plane charge transfer and T_c. At the same time, structural changes occur that are mainly responsible for the downshift of ω_{CF} in Fig. 4(a) (see above). For $Nd_{1+x}Ba_{2-x}Cu_3O_6$, the absence of chain oxygen (missing reservoirs) provides ''space'' to accomodate negative charge from the Nd ions that cannot be taken up by the CuO_2 planes since they are completely undoped. We thus conjecture that any structural changes also occur mainly in the empty chain region of the compound and that the geometry of the CuO_2 planes remains unaffected. Hence the CF level energy does not change with x. Structural data from neutron difraction would be very useful to futher investigate these phenomena.

V. CONCLUSIONS

We have performed a Raman study of the effects of Nd^{3+}/Ba^{2+} ion substitution on the coupled-phonon–CF-excitation structure in $Nd_{1+x}Ba_{2-x}Cu_3O_y$. We find that a decrease in the oxygen concentration y in samples without excess Nd ($x=0$) affects the unrenormalized B_{1g} phonon energy in a similar way as an increase of x in $Nd_{1+x}Ba_{2-x}Cu_3O_7$. The amount of phonon softening with temperature decreases with T_c, independent of the type of doping. The absence of phonon hardening in the underdoped region is consistent with a gap increase although T_c decreases. A possible relation between this gap and the so-called pseudogap must be left open at this point and will be subject of further investigation. Shifts of the bare CF level energy with doping are mainly related to structural changes in the CuO_2 planes, induced either by an excess of Nd^{3+} or by a decreasing oxygen content. We find no change in the bare CF level energy for oxygen-depleted $Nd_{1+x}Ba_{2-x}Cu_3O_6$, indicating the absence of structural changes in the CuO_2 planes with varying Nd content in this case.

ACKNOWLEDGMENTS

We thank V. I. Belitsky for fruitful discussions, H. Hirt and M. Siemers for technical assistance, and V. Hadjiev for a critical reading of the manuscript. One of the authors (A.A.M.) acknowledges the financial support from FAPESP-Brazil under Contract No. 96/06992-8.

[1] K. Takita, H. Katoh, H. Akinaga, M. Nishino, T. Ishigaki, and H. Asano, Jpn. J. Appl. Phys., Part 2 **27**, L57 (1988).

[2] K. Takita, H. Akinaga, H. Katoh, and K. Masuda, Jpn. J. Appl. Phys., Part 2 **27**, L607 (1988).

[3] M. J. Kramer, S. I. Yoo, R. W. McCallum, W. B. Yelon, H. Xie, and P. Allenspach, Physica C **219**, 145 (1994).

[4] P. Allenspach, J. Mesot, U. Staub, M. Guillaume, A. Furrer, S.-I. Yoo, M. J. Kramer, R. W. McCallum, H. Maletta, H. Blank, H. Mutka, R. Osborn, M. Arai, Z. Bowden, and A. D. Taylor, Z. Phys. B **95**, 301 (1994).

[5] E. Goodilin, M. Kambara, T. Umeda, and Y. Shiohara, Physica C **289**, 251 (1997).

[6] E. T. Heyen, R. Wegerer, and M. Cardona, Phys. Rev. Lett. **67**, 144 (1991).

[7] E. T. Heyen, R. Wegerer, E. Schönherr, and M. Cardona, Phys. Rev. B **44**, 10 195 (1991).

[8] P. Allenspach, A. Furrer, P. Bruesch, and P. Unternaehrer, Physica B **156-157**, 864 (1989).

[9] T. Ruf, Physica B **219**, 132 (1996).

[10] T. Strach, T. Ruf, A. M. Niraimathi, A. A. Martin, and M. Cardona, Physica C **301**, 9 (1998).

[11] B. Friedl, C. Thomsen, and M. Cardona, Phys. Rev. Lett. **65**, 915 (1990).

[12] C. Thomsen, M. Cardona, B. Friedl, C. O. Rodriguez, I. I. Mazin, and O. K. Andersen, Solid State Commun. **75**, 219 (1990); see also B. Friedl, dissertation, Universität Stuttgart, 1992.

[13] Th. Wolf, W. Goldacker, B. Obst, G. Roth, and R. Flükiger, J. Cryst. Growth **96**, 1010 (1989).

[14] H.-U. Habermeier, M. Cardona, V. G. Hadjiev, R. Gajic, and M. N. Iliev, Physica C **279**, 63 (1997).

[15] S. L. Cooper, M. V. Klein, B. G. Pazol, J. P. Rice, and D. M. Ginsberg, Phys. Rev. B **37**, 5920 (1988).

[16] R. Wegerer, C. Thomsen, T. Ruf, E. Schönherr, M. Cardona, M. Reedyk, J. S. Xue, J. E. Greedan, and A. Furrer, Phys. Rev. B **48**, 6413 (1993).

[17] The values for the coupling constant V shown in Fig. 9 of Ref. 16 are too large by a factor of $\sqrt{2}$ [see Eq. (3) of Ref. 7]. The values of V given in the text of Ref. 16, however, correspond to the definition of the coupled-excitation energies given in Eq. (3) of Ref. 16. This definition, corrected by the factor of $\sqrt{2}$, is also used in the present paper and in Ref. 10.

[18] R. Zeyher and G. Zwicknagl, Z. Phys. B **78**, 175 (1990).

[19] Ch. Renner, B. Revaz, J. -Y. Genoud, K. Kadowaki and Ø. Fischer, Phys. Rev. Lett. **80**, 149 (1998).
[20] N. Miyakawa, P. Guptasarma, J. F. Zasadzinski, D. G. Hinks, and K. E. Gray, Phys. Rev. Lett. **80**, 157 (1998).
[21] T. Ruf, C. Thomsen, R. Liu, and M. Cardona, Phys. Rev. B **38**, 11 985 (1988).
[22] M. C. Krantz, H. J. Rosen, R. M. Macfarlane, and V. Y. Lee, Phys. Rev. B **38**, 4992 (1988).
[23] E. Altendorf, J. C. Irwin, R. Liang, and W. N. Hardy, Phys. Rev. B **45**, 7551 (1992).
[24] N. Pyka, W. Reichardt, L. Pintschovius, G. Engel, J. Rossat-Mignod, and J. Y. Henry, Phys. Rev. Lett. **70**, 1457 (1993).
[25] M. T. Hutchings, Solid State Phys. **16**, 227 (1964).
[26] H. Shaked, B. W. Veal, J. Faber, Jr., R. L. Hitterman, U. Balachandran, G. Tomlins, H. Shi, L. Morss, and A. P. Paulikas, Phys. Rev. B **41**, 4173 (1990).
[27] By this procedure we take into account residual inaccuracies of the point-charge-model calculation (about 5%) in a phenomenological way. Note, however, that this does not affect relative changes of ω_{CF} due to doping.